Inorganic Chemistry

Article

pubs.acs.org/IC

Lattice Solvent and Crystal Phase Effects on the Vibrational Spectra of $UO_2Cl_4^{2-}$

David D. Schnaars and Richard E. Wilson*

Chemical Sciences and Engineering Division, Argonne National Laboratory, Argonne, Illinois 60439, United States

Supporting Information

ABSTRACT: We present the structural and spectroscopic characterization of six uranyl tetrachloride compounds along with a quantified analysis showing the influence of both the crystallographic phase and the lattice solvent upon the vibrational properties of the uranyl moiety. From the uranyl symmetric and asymmetric stretching frequencies we use a valence bond potential model to calculate the stretching and interaction force constants of the uranyl moiety in each compound. Quantifying these second-sphere influences provides insight into the vibrational properties, and indirectly the electronic structure, of the uranyl ion in its ground state. These data provide a better guide for assessing the validity of future comparisons with respect to bond strength, length, and electronic properties among series of actinyl compounds where non-actinide variables may be at play.

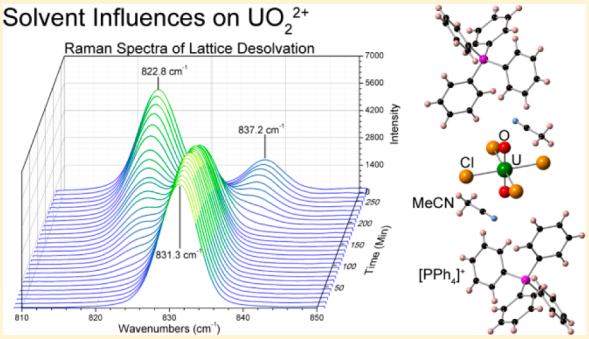

INTRODUCTION

The unique electronic properties of the actinides, specifically the energy levels of the 5f and 6d orbitals, give rise to their unique properties, such as their varying oxidation states, high coordination numbers, and increased covalent bonding in comparison to those of the lanthanides.[1,2] Since chemistry happens at the electronic level, understanding the electronic structure and how it influences and manifests itself in the chemistry and physical properties of these elements is vital in controlling their behavior during processes such as separations, waste remediation, and speciation in the environment. Due in part to the radiological hazards associated with the actinides and the controlled nature of the transuranic elements, our understanding of their chemistry significantly lags behind that of the other elements in the periodic table.[3,4]

In efforts to bridge this knowledge gap between the actinides and the rest of the periodic table, researchers have exploited the periodic trends across the actinide series to investigate the chemistry and electronic structure of these elements. One of the earliest implementations of chemical periodicity in the actinides led to the observations concerning metal−ligand bond lengths in the actinide dioxides that were crucial in Seaborg's proposal to place the actinide elements where they currently reside in the periodic table.[5−7] Since then, numerous experimental[8−25] and theoretical[10,12,14,16−19,26−29] studies looking at trends in the solid-state molecular structure, ligand coordination, and chemical properties across the series have provided valuable insight into the properties of the actinides.

While this approach works well when comparing systems that vary only by the identity of the metal center, it is sometimes difficult to decouple all of the contributing factors and determine if the root cause of differences are actinide-centric when comparing more complex systems. One example of this can be seen in our previous work, where we employed Raman and infrared spectroscopy to investigate the differences in electronic structure between uranyl and plutonyl using analogous $M_2AnO_2Cl_4$ compounds (An = U, Pu; M = Rb, Cs, Me_4N).[20] During our analysis of these compounds, we were unable to directly compare the rubidium analogues because, in addition to varying the actinide metal center, these compounds also crystallized in different space groups and solvation states, $Rb_2UO_2Cl_4{\cdot}2H_2O$ ($P\bar{1}$) and $Rb_2PuO_2Cl_4$ ($C2/m$). Without knowing how variations in the crystallographic phase and solvent state affected the vibrational spectroscopy—the so-called matrix effects—we were unable to conclusively attribute the spectroscopic differences to metal-centric changes in the vibrational spectra of the actinyl.

The primary goal of this article is to utilize our unique series of homologous $[PPh_4]_2UO_2Cl_4{\cdot}x$solvent compounds to demonstrate and quantify the influences of crystallographic phase and lattice solvent on the vibrational properties of the uranyl moiety. A better experimental understanding and demonstration of how the crystallographic phase and lattice solvent affect the metal center could help improve future theoretical calculations for the actinides, highlighting the necessity of considering second coordination sphere and higher effects on the calculated properties of molecular species. Quantifying these influences gives insight into the electronic structure of the uranyl ion and provides a better guide for assessing the validity

Received: July 1, 2014
Published: October 9, 2014

   dx.doi.org/10.1021/ic501553m | *Inorg. Chem.* 2014, 53, 11036−11045

Table 1. X-ray Crystallographic Data for Complexes 1−6

	1	2	3	4	5	6
empirical formula	$Cl_4H_{40}C_{48}O_2P_2U$	$Cl_4H_{40}C_{48}O_2P_2U$	$Cl_8H_{44}C_{50}O_2P_2U$	$Cl_4H_{46}C_{52}O_2N_2P_2U$	$Cl_{12}H_{132}C_{147}O_9P_6U_3$	$Cl_8H_{44}C_{50}O_2As_2U$
crystal habit	irregular	irregular	prismatic	block	prismatic	prismatic
crystal color	yellow/green	yellow/green	yellow/green	yellow/green	yellow/green	yellow/green
crystal size (mm)	0.15 × 0.14 × 0.10	0.16 × 0.09 × 0.06	0.51 × 0.16 × 0.11	0.17 × 0.09 × 0.09	0.32 × 0.22 × 0.19	0.34 × 0.25 × 0.12
crystal system	triclinic	monoclinic	triclinic	triclinic	monoclinic	triclinic
space group	$P\bar{1}$	$P2_1/c$	$P\bar{1}$	$P\bar{1}$	$P2_1/c$	$P\bar{1}$
volume (Å^3)	1083.99(11)	2247.3(2)	1258.5(2)	1228.58(14)	6860.8(9)	1289.0(2)
a (Å)	10.0272(6)	12.9364(8)	10.0361(11)	10.1875(7)	25.7235(19)	10.1478(9)
b (Å)	10.0808(6)	10.7145(6)	10.9404(12)	10.9670(7)	15.9920(12)	11.0220(10)
c (Å)	12.0598(7)	19.5933(9)	12.6063(14)	12.5027(8)	16.7783(12)	12.6883(12)
α (deg)	99.6630(10)	90	69.1770(10)	65.3610(10)	90	69.2140(10)
β (deg)	93.3890(10)	124.158(3)	76.9480(10)	84.7350(10)	96.2670(10)	76.7240(10)
γ (deg)	114.3080(10)	90	82.5430(10)	75.4030(10)	90	82.1540(10)
Z	1	2	1	1	2	1
formula weight (g/mol)	1090.57	1090.57	1260.42	1172.68	3367.84	1348.32
density (calcd) (Mg/m^3)	1.671	1.612	1.663	1.585	1.630	1.737
absorption coefficient (mm^{-1})	4.103	3.958	3.752	3.627	3.893	4.874
F_{000}	534	1068	618	578	3312	654
total no. reflections	15401	31504	15445	20344	83296	20626
unique reflections	5971	6490	5776	8403	15759	8433
final R indices [$I > 2\sigma(I)$]	R_1 = 0.0257, wR_2 = 0.0540	R_1 = 0.0272, wR_2 = 0.0517	R_1 = 0.0209, wR_2 = 0.0498	R_1 = 0.0276, wR_2 = 0.0524	R_1 = 0.0258, wR_2 = 0.0562	R_1 = 0.0276, wR_2 = 0.0623
largest diff. peak and hole (e$^-$ Å^{-3})	1.637 and −0.470	0.725 and −0.621	1.287 and −0.805	0.860 and −0.522	1.094 and −0.894	1.675 and −1.078
GOF	1.042	1.011	1.069	1.040	1.016	1.024

of future comparisons among series of actinyl compounds where non-actinide variables may be at play. To this end, we have studied a series of uranyl complexes using Raman and infrared spectroscopy to examine differences in the symmetric (ν_1) and asymmetric (ν_3) stretching modes of the $UO_2Cl_4^{2-}$ anion as a function of crystallographic phase and the presence of lattice solvent among $[PPh_4]_2UO_2Cl_4{\cdot}x$solvent compounds. The observed differences are then quantified using a harmonic valence bond potential model to calculate the stretching (k_1) and interactive (k_{12}) force constants for the uranyl moiety in each compound. Finally, the synthesis of isostructural compounds $[PPh_4]_2UO_2Cl_4{\cdot}2CH_2Cl_2$ and $[AsPh_4]_2UO_2Cl_4{\cdot}2CH_2Cl_2$ allows us to investigate the influence of the central atom of the cation on the observed vibrational spectra of the uranyl moiety.

Herein, we present the structural and spectroscopic characterization of six uranyl tetrachloride compounds along with an analysis demonstrating the influence of both crystallographic phase and lattice solvent on the vibrational spectra of the uranyl moiety. Subsequently, applying the results of this study to the data from our previous work allows us to make some qualitative assessments of the spectroscopic data for the rubidium analogues, $Rb_2UO_2Cl_4{\cdot}2H_2O$ ($P\bar{1}$) (**U-Rb**) and $Rb_2PuO_2Cl_4$ ($C2/m$) (**Pu-Rb**), which differ from each other by actinide metal, space group, and the presence of lattice solvent.[20] Additionally, our results demonstrate that some caution must be employed when comparing the vibrational frequencies of actinyl complexes, especially when employing empirical relationships between vibrational frequencies, bond lengths, and bond strengths.

EXPERIMENTAL SECTION

Caution! *Depleted uranium is an α-emitting radionuclide, and standard precautions for handling radioactive materials should be observed when performing the following synthetic procedures. The following reactions were performed under ambient conditions, and unless otherwise noted, all materials with the exception of depleted uranium were obtained from commercial sources and used as received. KBr was ground and dried for a minimum of 48 h at 120 °C before use.*

Vibrational Spectroscopy. Infrared samples were diluted (∼1−5 wt %) with dry KBr and pressed into a pellet before being collected on a Nicolet Nexus 870 FTIR system. Data were collected using 16 scans over 4000−400 cm^{-1} with a resolution of 2 cm^{-1}. ATR data were collected on crushed single crystals using a Nicolet Nexus 870 FTIR system with Smart DuraSamplIR stage. Data were collected using 16 scans over 4000−400 cm^{-1} with a resolution of 2 cm^{-1}. Raman data were collected on randomly oriented single crystals using a Renishaw inVia Raman microscope with a circularly polarized excitation line of 785 nm. To prevent desolvation and degradation of compounds **3**−**6** during Raman analysis, crystals were placed in a capillary tube along with a portion of the mother liquor and sealed with modeling clay to ensure a solvent-rich atmosphere.

X-ray Crystallography. The solid-state molecular structures for complexes **1**−**6** were determined similarly, with exceptions noted. Crystals were mounted on a glass fiber under Paratone-N oil. Hemispheres of data (0.5° frame widths) were collected using a Bruker SMART or QUAZAR diffractometer equipped with an APEXII detector using Mo Kα radiation. Frame exposures of 30, 45, 20, 40, 15, and 20 s were used for compounds **1**−**6**, respectively. All data were collected at 100 K using an Oxford Cryosystems cryostat. The data were integrated and corrected for absorption using the APEX2 suite of crystallographic software, while structure solutions and refinements were completed using XShell.[30]

Table 1 summarizes the X-ray crystallographic data for compounds **1**−**6**.

General Synthesis for Compounds 1−6. Compounds **1**−**6** were all synthesized following a similar procedure (a detailed synthesis for each compound along with isolated yields can be found in the Supporting Information). In each case, dissolution of UO_3 in 2.0 M HCl followed by layering with an organic solution of $[PPh_4]Cl$ (**1**−**5**) or $AsPh_4$ (**6**) results in the extraction of uranium into the organic phase, presumably as a uranyl chloride species. This is observed

dx.doi.org/10.1021/ic501553m | Inorg. Chem. 2014, 53, 11036−11045

visually by the transfer of color from the aqueous to organic phase over a period of a few minutes. Evaporation of the solution at room temperature leads to the deposition of $R_2UO_2Cl_4{\cdot}x$solvent as a yellow-green crystalline material in moderate to good yield [R = PPh_4, x = 0 (**1** and **2**), solvent = acetone; R = PPh_4, x = 2, solvent = CH_2Cl_2 (**3**); R = PPh_4, x = 2, solvent MeCN (**4**); R = PPh_4, x = 1, solvent = MeOH (**5**); R = $AsPh_4$, x = 2, solvent = CH_2Cl_2 (**6**)].

RESULTS

Synthesis and Structural Descriptions. Dissolution of UO_3 in 2.0 M HCl followed by layering with an organic solution of $[PPh_4]Cl$ (**1**–**5**) or $AsPh_4$ (**6**) leads to the deposition of $R_2UO_2Cl_4{\cdot}x$solvent as a yellow-green crystalline material in moderate to good yield [R = PPh_4, x = 0 (**1** and **2**), solvent = acetone; R = PPh_4, x = 2, solvent = CH_2Cl_2 (**3**); R = PPh_4, x = 2, solvent MeCN (**4**); R = PPh_4, x = 1, solvent = MeOH (**5**); R = $AsPh_4$, x = 2, solvent = CH_2Cl_2 (**6**)]. This simple solvent extraction is a useful pathway for the synthesis of anhydrous uranyl tetrachloride, which, as mentioned by Spencer et al., can be utilized as a potential starting material for both aqueous and nonaqueous uranyl chemistry.[31−34] Unlike some previous procedures,[34] our synthesis allows for the room-temperature formation of anhydrous $[PPh_4]_2UO_2Cl_4$ directly from UO_3 without the need for dry solvents or an inert atmosphere. Additionally, the $[PPh_4]^+$ cation increases the solubility of the $UO_2Cl_4^{2-}$ anion in organic solvents in comparison to the alkali metal analogues such as $Rb_2UO_2Cl_4{\cdot}2H_2O$ and $Cs_2UO_2Cl_4$.[35−37] In our studies, the anion−cation pair of compounds **1**–**6** appear to be stable in the solid state under atmospheric conditions, with the only noticeable degradation being the desolvation of the lattice solvent over time for compounds **3**, **4**, and **6**, as demonstrated below by vibrational spectroscopy.

It should be noted that the solid-state molecular structure for the monosolvate of **3**, $[PPh_4]_2UO_2Cl_4{\cdot}CH_2Cl_2$, has been previously reported.[38] This species was isolated as the secondary product from the reaction to form $(PPh_4)UOCl_4$-{NP-(*m*-tol)$_3$} and crystallizes in the triclinic space group $P\bar{1}$. In addition to the monosolvate, the solid-state molecular structure for the bromo analogue of compound **3**, $[PPh_4]_2UO_2Br_4{\cdot}2CH_2Cl_2$, has also been reported.[39] This compound is the oxidation product of $[PPh_4]_2U_2Br_{10}$ and crystallizes in the monoclinic space group $C2/c$.[39] Finally, the iodo analogue of **4**, $[PPh_4]_2UO_2I_4{\cdot}2$MeCN, has also been structurally characterized and crystallizes in the monoclinic space group $C2/c$.[40]

Complexes **1**–**6** crystallize in either the triclinic space group $P\bar{1}$ (**1**, **3**, **4**, and **6**) or the monoclinic space group $P2_1/c$ (**2** and **5**) (Table 1). In each case, the composition of the anion is identical, consisting of a linear uranyl moiety with four chloride ligands bound in the equatorial plane, forming a pseudo-octahedral geometry (Figure 1). The average lengths of the U═O and U—Cl bonds for complexes **1**–**6** are 1.773(4) and 2.670(8) Å, respectively (Table 2), which are consistent with previously reported uranyl tetrachloride compounds containing cations such as Rb, Cs, Me_4N, Et_4N, $[(NH_4)(5\text{-crown-}5)_2]$, and $SN_2C_{10}H_9$ (U═O: 1.751(9)−1.776(6) Å; U−Cl: 2.644(3)−2.682(2) Å).[20,35,37,41−43]

All of the complexes presented in this study crystallize in centrosymmetric space groups with the uranium atom residing on a special position with inversion symmetry, resulting in a strictly linear conformation of the uranyl moiety. The only exception to this is found in compound **5**, where two crystallographically distinct anions are present in the unit cell.

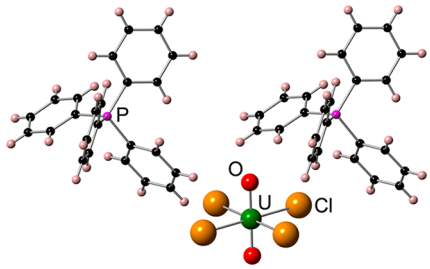

Figure 1. Ball-and-stick model of $[PPh_4]_2UO_2Cl_4$ (**1**) depicting the connectivity around the metal center and charge-balancing cations (U = green, Cl = orange, O = red, P = pink, C = black, H = beige).

Table 2. Selected Bond Lengths for Complexes 1−6

	U═O (Å)	U—Cl (Å)
$[PPh_4]_2UO_2Cl_4$ ($P\bar{1}$) (**1**)	1.776(2)	2.669(1)
		2.686(1)
$[PPh_4]_2UO_2Cl_4$ ($P2_1/c$) (**2**)	1.776(2)	2.654(1)
		2.670(1)
$[PPh_4]_2UO_2Cl_4{\cdot}2CH_2Cl_2$ (**3**)	1.770(2)	2.663(1)
		2.666(1)
$[PPh_4]_2UO_2Cl_4{\cdot}2$MeCN (**4**)	1.772(1)	2.671(1)
		2.673(1)
$[PPh_4]_2UO_2Cl_4{\cdot}$MeOH (**5**)	1.775(2)	2.670(1)
	1.764(2)	2.674(1)
	1.774(2)	2.662(1)
		2.667(1)
		2.675(1)
		2.686(1)
$[AsPh_4]_2UO_2Cl_4{\cdot}2CH_2Cl_2$ (**6**)	1.774(2)	2.668(1)
		2.669(1)
average (SD)[44]	**1.773(4)**	**2.670(8)**

The first anion, U2, sits on a crystallographic inversion center, while the second crystallographically unique uranyl anion (U1) resides on a general position and has an O═U═O bond angle of 178.72(9)°.

For each compound, the uranyl anion is charge-balanced by the presence of two monocations, PPh_4^+ for compounds **1**–**5** and $AsPh_4^+$ for compound **6**. In each case, the solid-state molecular structures show that the phenyl substituents of the cations are arranged in a pseudotetrahedral geometry around the central atom. The hydrogen atoms associated with the phenyl rings of the cations in compounds **1**–**6** appear to interact with both the oxo and chloride ligands of the actinyl anion. The shortest C−H···O_{yl} and C−H···Cl interactions within each solid-state molecular structure range from 2.34(3) (**5**) to 2.64 Å (**1**) and from 2.68(4) Å (**6**) to 2.83(3) Å (**5**), respectively (Table 3, Figure 2). While the C−H···O_{yl} distances are longer than previously reported hydrogen-bonding interactions involving the uranyl oxo ligand (ranging from 1.665(13) to 2.39(3) Å),[45] these distances are consistent with values previously reported for $[PPh_4]^+$ interactions with metal-bound oxide and chloride ligands, where the mean (PPh_4)C−H···O_M distance is 2.7004 Å[46] and the mean C−H···Cl_M interaction is 2.876 Å.[47] We expect these anion−cation

dx.doi.org/10.1021/ic501553m | Inorg. Chem. 2014, 53, 11036−11045

Table 3. Shortest Cation−Anion and Solvent−Anion Interactions for Complexes 1−6

cation/compound		cation···O_{yl} interactions		cation···Cl interactions		solvent···anion interactions
PPh_4, $AsPh_4$		H···O_{yl} (Å)	C−H···O_{yl} (deg)	H···Cl (Å)	C−H···Cl (deg)	H···Cl (Å)
1 ($P\bar{1}$)[a]		2.64	145.1	2.77	129.6	
2 ($P2_1/c$)[a]		2.44	148.3	2.75	148.4	
3		2.60(3)	134(2)	2.75(3)	133(2)	2.64(3) (CH_2Cl_2)
4		2.56(2)	136(2)	2.79(3)	165(2)	2.77(3) (MeCN)
5	U1	2.39(4)	159(3)	2.69(3)	153(2)	2.49 (Me*OH*)[a]
	U2	2.34(3)	137(3)	2.83(3)	143(2)	
6		2.55(3)	136(3)	2.68(4)	142(3)	2.64(4) (CH_2Cl_2)

[a]No ESDs due to a constraint on the hydrogen atom bond distances within the solid-state refinement model.

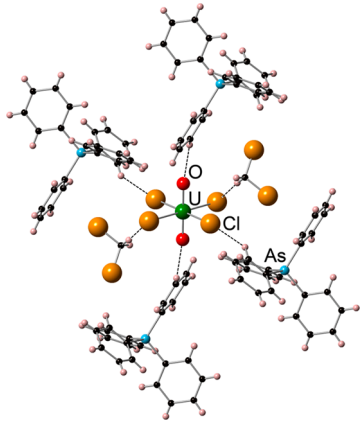

Figure 2. Ball-and-stick model showing the hydrogen-bonding interactions in $[AsPh_4]_2UO_2Cl_4{\cdot}2CH_2Cl_2$ (**6**). Dashed lines indicate cation−anion and solvent−anion hydrogen-bonding interactions (U = green, Cl = orange, O = red, As = light blue, C = black, H = beige).

interactions to be relatively weak, in part due to the longer distance associated with these hydrogen-bonding interactions in comparison to previously reported hydrogen-bonding interactions with uranyl and the relatively large size of the $[RPh_4]^+$ cations, where the single cationic charge is spread out over the central atom and four phenyl groups.

In addition to the anion and cations found in the unit cell, complexes **3**−**6** also contain unbound solvent within the crystal lattice. In these complexes, none of the solvent molecules interact with the oxo ligand of the -yl moiety, but they do appear to interact with the equatorial chloride ligands (Table 3). Complexes **3** and **6** both contain CH_2Cl_2 within the crystal lattice. For compound **3**, the $C_{solvent}$···Cl distance is 3.527(3) Å and the $C_{solvent}$−H···Cl distance is 2.64(3) Å, both of which are consistent with reported hydrogen-bonding interactions for CH_2Cl_2.[48] For compound **6**, the analogous interactions are statistically identical (3σ) to those found in **3**, the $C_{solvent}$···Cl and $C_{solvent}$−H···Cl distances being 3.539(3) and 2.64(4) Å, respectively (Figure 2). Similar interactions are also observed in compound **4** between the anion and the MeCN solvent, with a $C_{solvent}$−H···Cl distance of 2.77(3) Å and a $C_{solvent}$···Cl separation of 3.647(3) Å.[49,50] Compound **5** contains solvent−anion interactions with $O_{solvent}$···Cl and $O_{solvent}$−H···Cl distances of 3.285(2) and 2.49 Å (Me*OH*), respectively. Unlike compounds **3**, **4**, and **6**, the solvent−anion distances for compound **5** are significantly longer than the reported average $O_{solvent}$···Cl and $O_{solvent}$−H···Cl hydrogen-bonding interactions for C(sp^3)*OH* (3.100(4) and 2.150(5) Å).[48] The longer than average distances for this compound suggests that these are relatively weaker hydrogen-bonding interactions between the solvent and anion in compound **5** than those seen in compounds **3**, **4**, and **6**.

Vibrational Spectroscopy. In addition to single-crystal X-ray diffractometry, complexes **1**−**6** have also been characterized using Raman and infrared spectroscopy. Previous reports on $[PPh_4]_2UO_2Cl_4$ have assigned the symmetric and asymmetric stretching frequencies of the uranyl moiety as well as a few of the Raman- and infrared-active metal−chloride vibrations, but, to our knowledge, these assignments were not correlated to a known crystallographic phase or solvation state of the compound.[51,52]

As discussed in our previous work,[20] the vibrational spectra of the uranyl moiety can be interpreted in the linear $D_{\infty h}$ geometry with three normal modes of vibration. These modes include the symmetric stretching mode (ν_1, Raman active), a doubly degenerate bending mode (ν_2, IR active), and the asymmetric stretching mode (ν_3, IR active).[53] Of these three modes, our discussion here will focus primarily on the symmetric and asymmetric vibrations, which are typically observed for uranyl in aqueous solution between 860−880 (ν_1) and 930−960 cm^{-1} (ν_3), respectively.[54] We will not discuss the bending mode (199−210 cm^{-1})[54] because it lies outside the wavelength limitations of our infrared spectrometer.

For compounds **1**−**6**, the uranyl symmetric stretch (ν_1) is a prominent signal in the Raman spectra located between 820 and 840 cm^{-1} (Table 4) (Figure 3). With the exception of compound **2** (823(1) cm^{-1}), the observed symmetric stretching frequencies for compounds **1**−**6** agree well with the range of literature values for the $UO_2Cl_4^{2-}$ anion (831−842 cm^{-1}).[55−62] The asymmetric stretching mode (ν_3) for complexes **1**−**6** appears as a strong absorption between 900 and 920 cm^{-1} (Table 4, Figure 3). Similar to the symmetric vibrational mode, the observed frequency range for the asymmetric stretching frequency lies within the range of values previously reported for

Table 4. Symmetric (ν_1, cm^{-1}) and Asymmetric (ν_3, cm^{-1}) -yl Stretches for Complexes 1−6 Along with the Stretching Force Constant (k_1, mdyn/Å) and Interaction Force Constant (k_{12}, mdyn/Å) for the O=An=O bond

compound	ν_1	ν_3	k_1	k_{12}
UO_2^{2+}(aq)	860−880[54]	930−960[54]		
$[PPh_4]_2UO_2Cl_4$ ($P\bar{1}$) (**1**)	838(1)	919(1)	6.82	−0.20
$[PPh_4]_2UO_2Cl_4$ ($P2_1/c$) (**2**)	823(1)	904(1)	6.58	−0.20
$[PPh_4]_2UO_2Cl_4{\cdot}2CH_2Cl_2$ (**3**)	833(1)	912(1)	6.72	−0.19
$[PPh_4]_2UO_2Cl_4{\cdot}2MeCN$ (**4**)	832(1)	911(1)	6.71	−0.19
$[PPh_4]_2UO_2Cl_4{\cdot}MeOH$ (**5**)	836(1)	914(1)	6.76	−0.18
$[AsPh_4]_2UO_2Cl_4{\cdot}2CH_2Cl_2$ (**6**)	834(1)	912(1)	6.73	−0.18

dx.doi.org/10.1021/ic501553m | Inorg. Chem. 2014, 53, 11036−11045

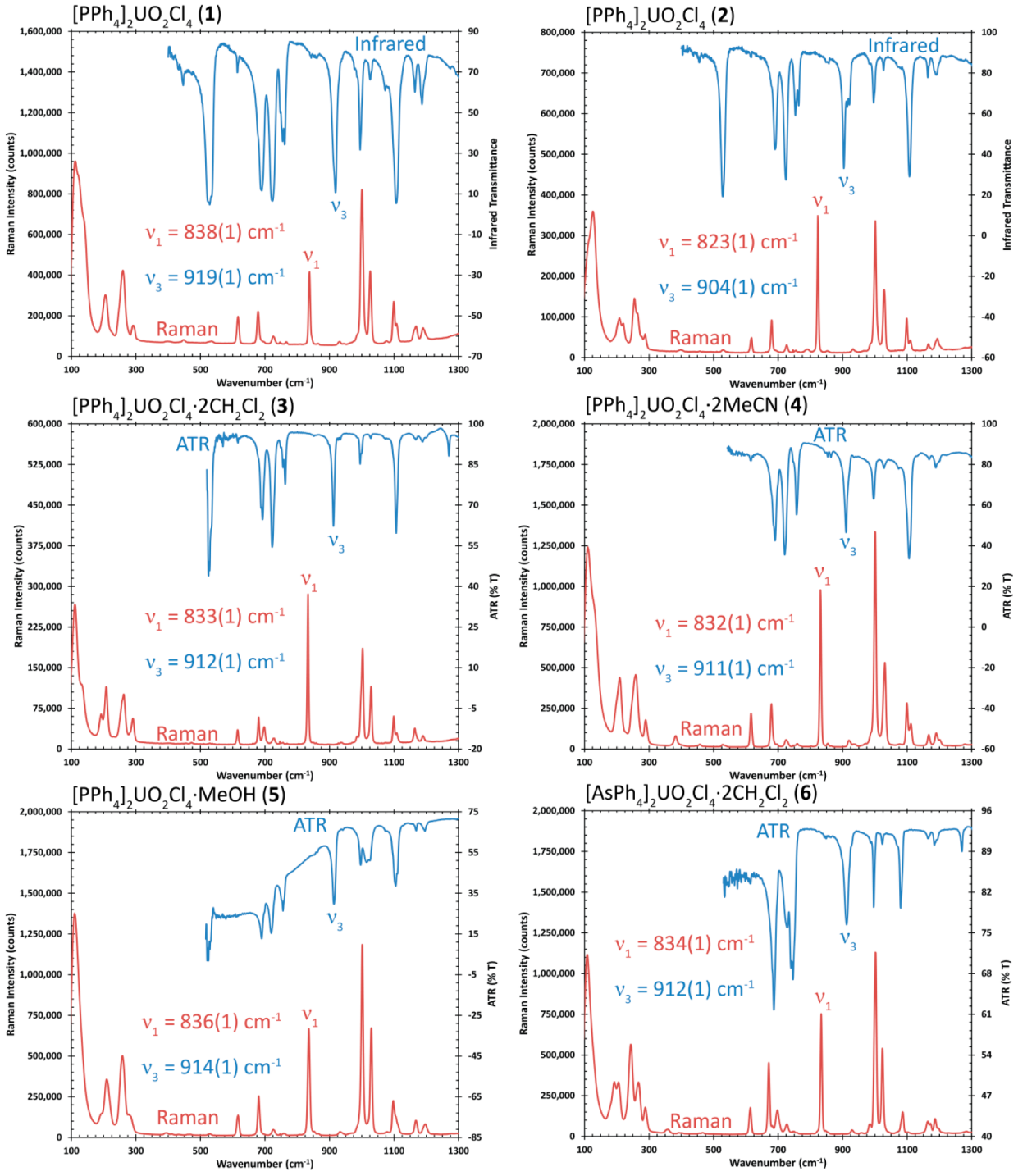

Figure 3. Infrared/ATR (blue) and Raman (red) spectra for $[PPh_4]_2UO_2Cl_4$ ($P\bar{1}$) (**1**) (upper left), $[PPh_4]_2UO_2Cl_4$ ($P2_1/c$) (**2**) (upper right), $[PPh_4]_2UO_2Cl_4{\cdot}2CH_2Cl_2$ (**3**) (middle left), $[PPh_4]_2UO_2Cl_4{\cdot}2MeCN$ (**4**) (middle right), $[PPh_4]_2UO_2Cl_4{\cdot}MeOH$ (**5**) (lower left), $[AsPh_4]_2UO_2Cl_4{\cdot}2CH_2Cl_2$ (**6**) (lower right).

uranyl tetrachloride compounds (900−922 cm^{-1}).[55−58,60−62] The ∼20 cm^{-1} distribution of frequencies for both the symmetric and asymmetric stretching modes of compounds **1**−**6** is most likely due to variations in the crystallographic phase and the presence of lattice solvent, a theory that is addressed further below.

Interestingly, the symmetric and asymmetric stretches of $(PPh_4)_2UO_2Cl_4{\cdot}2MeCN$ (**4**) are very similar to those of the analogous iodo compound $(PPh_4)_2UO_2I_4{\cdot}2MeCN$.[40] For the iodo species, the ν_1 vibrational mode is identical to that of the chloride species observed at 832 cm^{-1}, while the ν_3 signal is blue-shifted by only 5 cm^{-1}, appearing at 915 cm^{-1}. These similar vibrational frequencies between the uranyl chloro and iodo analogues are somewhat surprising, considering the differing equatorial ligands. It might be expected that the change of the halide from chloride to iodide would result in differing vibrational frequencies, based on differences in the hardness of the anions. However, this is not observed to be the case. The observed vibrational frequencies are likely influenced by their different crystalline phases: the two compounds

dx.doi.org/10.1021/ic501553m | Inorg. Chem. 2014, 53, 11036−11045

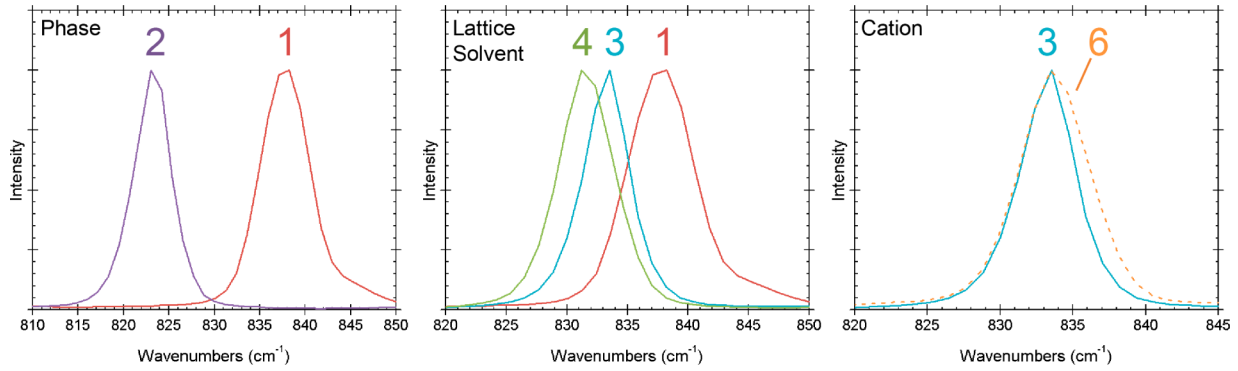

Figure 4. Raman spectra showing the uranyl symmetric stretching frequency for $[PPh_4]_2UO_2Cl_4$ ($P\bar{1}$) (**1**, red), $[PPh_4]_2UO_2Cl_4$ ($P2_1/c$) (**2**, purple), $[PPh_4]_2UO_2Cl_4{\cdot}2CH_2Cl_2$ (**3**, teal), $[PPh_4]_2UO_2Cl_4{\cdot}2MeCN$ (**4**, green), and $[AsPh_4]_2UO_2Cl_4{\cdot}2CH_2Cl_2$ (**6**, orange dashed line). The spectra in the left plot are of compounds where only the crystallographic phase differs. The spectra in the middle plot are of compounds that differ only by the presence of lattice solvent. The spectra in the right plot are of isostructural compounds with only minor differences in the cation. All spectra are normalized to the uranyl symmetric stretch.

crystallize in different space groups (**4**: triclinic $P\bar{1}$; iodo analogue: monoclinic $C2/c$),[40] an observation that we attribute to the significant shift of the uranyl vibration between compounds **1** and **2**.

It is worth noting that, while vibrational frequencies have been used as indicators for both the An=O bond length and the degree of influence the equatorial ligands have upon the actinyl moiety, our Discussion section will show that the symmetric and asymmetric stretches are affected by a number of other factors as well. This means that correlations of vibrational frequencies to actinyl bond lengths and comparisons of stretching frequencies between compounds must be made carefully, making sure to take into account a variety of influencing factors beyond the first coordination sphere of the actinyl ion.

Stretching Force Constant. In an effort to quantify the differences among the vibrational spectra of the uranyl moieties in compounds **1**–**6**, we have calculated the stretching force constant (k_1) and interaction force constant (k_{12}) from the symmetric (ν_1) and asymmetric (ν_3) stretching frequencies as discussed in our previous work.[20] In a linear centrosymmetric triatomic molecule like uranyl, the stretching force constant describes the uranyl U=O bond, while the interaction force constant quantifies the interaction between the two uranyl oxygen atoms. The stretching force constants for compounds **1** and **2** are 6.82 and 6.58 mdyn/Å, respectively, while the four compounds containing lattice solvent (**3**–**6**) fall between 6.71 and 6.76 mdyn/Å (Table 4). These values are consistent with previously reported uranyl stretching force constants that were derived from both the symmetric and asymmetric stretching frequencies, such as in $(Me_4N)_2UO_2Cl_4$,[20] $[thiamine]_2UO_2Cl_4$,[63] and UO_2CO_3 (Rutherfordine),[64] which range from 6.45 to 7.92 mdyn/Å. In comparison to the stretching force constants, the interaction force constants for compounds **1**–**6** show much less variation, spanning only 0.2 mdyn/Å, from −0.18 to −0.20 mdyn/Å (Table 4). This narrow distribution of the interaction force constants for compounds **1**–**6** is smaller than the range of values we observed between $Rb_2UO_2Cl_4{\cdot}2H_2O$ (−0.10 mdyn/Å) and $Cs_2UO_2Cl_4$ (−0.27 mdyn/Å) but still consistent with those of previously reported uranyl compounds.[20,63,64] It is interesting to note that, while the stretching force constant describing the U=O interaction displays some variance between compounds, the near invariance of the interaction force constant indicates that the interaction between the two oxo ligands is relatively consistent.

DISCUSSION

Crystallographic Phase, Lattice Solvent, and Cation Influences on the Vibrational Spectra of the -yl Moiety. The complexes reported here provide a unique opportunity to directly examine the influence of crystallographic phase, lattice solvent, and variations of the cation upon the vibrational spectra of the uranyl moiety. To investigate these influences, we will make three comparisons of the compounds. First, to examine the effects of crystallographic phase upon the uranyl moiety we will look at compounds **1** and **2**, which vary only by their crystallographic space group and intermolecular arrangement. Second, a comparison of compounds **1**, **3**, and **4** will allow us to analyze isostructural compounds that vary only by the presence of lattice solvent in the solid-state molecular structure. Finally, comparing isostructural compounds **3** (PPh_4) and **6** ($AsPh_4$) gives us an opportunity to probe the sensitivity of this technique and assess the ability of Raman and infrared spectroscopy to detect different influences upon the vibrational spectra of the uranyl moiety due to a minor variation in the cation.

Our first analysis compares compounds **1** and **2**, both of which are unsolvated and have the chemical formula $[PPh_4]_2UO_2Cl_4$ but crystallize in different space groups. Due to their identical chemical formulas, these two compounds allow us to investigate the influence of crystallographic phase and intermolecular arrangement on the vibrational properties of the uranyl moiety. Compound **1** crystallizes in the triclinic space group $P\bar{1}$, while the solid-state molecular structure of compound **2** is observed in the monoclinic space group $P2_1/c$. The Raman spectrum for compound **1** shows the symmetric stretching frequency at 838(1) cm^{-1}, and the infrared spectrum displays the asymmetric stretch at 919(1) cm^{-1}. Both of these stretches are red-shifted in compound **2**, appearing at 823(1) and 904(1) cm^{-1} for the symmetric and asymmetric stretches, respectively (Figure 4). While the stretching force constant for **2** (6.58 mdyn/Å) is 0.24 mdyn/Å less than it is for **1** (6.82 mdyn/Å), the interaction force constants for both compounds are identical at −0.20 mdyn/Å (Table 4).

Because compounds **1** and **2** are polymorphs, the differences in the uranyl vibrations and the stretching force constant between the two species can be attributed to differences in the

dx.doi.org/10.1021/ic501553m | Inorg. Chem. 2014, 53, 11036−11045

crystallographic phase and intermolecular arrangement. In attempts to identify included disordered solvent molecules that would not be easily identified using X-ray crystallography, we also prepared these complexes from deuterated solvents, D_2O and d_6-acetone, and observed no differences in the vibrational spectra of the deuterated and protiated preparations. This indicates that, at least at the limits detectable by IR and Raman spectroscopy, the two preparations are not solvates.

There are a number of differences in the molecular arrangement of the two phases that might affect the vibrational properties of the uranyl moiety. As previously mentioned, one difference is the hydrogen-bonding interactions between the anion and cation (Figure S2). Another difference is observed when comparing the U−Cl bonds in the equatorial plane of the two compounds, which reveals that the average U−Cl bond length decreases by 0.016 Å when going from **1** to **2**.

One theory that could explain why the shorter U−Cl bond lengths result in red-shifting of the uranyl vibrational modes and a decrease in the stretching force constant is centered around electrostatic interactions.[65−70] In this theory, electrostatic interactions between the negatively charged Cl^- and O^{2-} ligands combined with the transfer of electron density from the equatorial ligands to the metal center result in destabilization of the An═O bonds.[70] The resulting destabilization can be observed as perturbations in the actinyl vibrational frequencies, which shift to lower wavenumbers as the bond weakens. This theory was recently supported by Vallet et al. in their theoretical study where they used a point-charge model to show that electrostatic interactions play a significant role in the equatorial ligand's influence upon the bonding within the uranyl moiety.[70]

The structural parameters of compounds **1** and **2** support the electrostatic theory as a cause for the perturbation to the U═O vibrational frequency because compound **2**, with the shorter U−Cl bond (more electronegativity at the metal center), also has the lower actinyl stretching frequencies. Although we cannot determine in our studies how these differences in the intermolecular arrangement of the two phases affect the electronic properties of the uranyl moiety, their influences on the vibrational spectra can be observed by comparing the symmetric and asymmetric stretching frequencies of **1** to **2**, each of which red-shifts by 15 cm^{-1} upon transitioning from $P\bar{1}$ to $P2_1/c$.

Our second comparison looks at the effects of lattice solvent on the vibrational spectra of the uranyl moiety. Compounds **1**, **3**, and **4** all contain the same cation−anion pair and crystallize in the triclinic space group $P\bar{1}$ with similar lattice parameters. The primary difference between these compounds is the presence of lattice solvent in the solid-state molecular structures of **3** ($2CH_2Cl_2$) and **4** (2MeCN), while the crystal lattice of compound **1** is unsolvated. The symmetric/asymmetric stretching frequencies of compounds **3** and **4** are located at 833(1)/912(1) cm^{-1} and 832(1)/911(1) cm^{-1}, respectively. In each case, the ν_1 and ν_3 signals are red-shifted from those of the unsolvated species (**1**), which appear at 838(1) and 919(1) cm^{-1}, respectively (Figure 4). Consistent with the red-shift observed for the symmetric and asymmetric stretching frequencies, the stretching force constant for the uranyl moiety decreases slightly when going from **1** (6.82 mdyn/Å) to **3** (6.72 mdyn/Å) to **4** (6.71 mdyn/Å) (Table 4). While the stretching force constants (k_1) for these three compounds span 0.09 mdyn/Å, the interaction force constants (k_{12}) are grouped over a much smaller range of only 0.01 mdyn/Å (**1**, −0.20; **3**, −0.19; **4**, −0.19 mdyn/Å) The 0.24 mdyn/Å difference between the two phases is more than twice as large as the 0.09 mdyn/Å range observed when examining the effects of lattice solvation, indicating that in this system the crystallographic phase may have a greater influence upon the observed vibrational spectra of the uranyl moiety than the presence of lattice solvent.

As with our discussion of phase differences, electrostatic interactions can also help explain why the solvent−anion interactions result in red-shifting of the uranyl vibrational modes and, in turn, a decrease in the stretching force constant. The hydrogen-bonding between the solvent and the chloride ligand could increase the electronegativity of the chloride or its donation of electron density into the metal center. This would in turn weaken the uranyl bonding, resulting in a red-shift of the symmetric and asymmetric stretches. Such hydrogen-bonding interactions were hypothesized to have similar effects in a series of plutonyl(VI) complexes that we studied previously.[71]

Finally, by comparing compounds **3** and **6**, we can investigate if minor cationic changes impart an influence upon the vibrational spectra of uranyl that is detectable by Raman and infrared spectroscopy in the solid state. These two compounds both crystallize in the triclinic space group $P\bar{1}$ with similar unit cells and contain isostructural $UO_2Cl_4^{-2}$ anionic units. The only difference between the two species is that compound **3** has PPh_4^+ as a cation, while compound **6** contains $AsPh_4^+$. As we saw in our previous work when using alkali metal cations,[20] as well as protonated pyridines,[71] the identity of the cation influences the vibrational properties of the actinyl moiety, as demonstrated through shifts in the symmetric and asymmetric stretching modes. One example of this is seen when comparing $Rb_2PuO_2Cl_4$ with $Cs_2PuO_2Cl_4$. While both compounds crystallize in the same space group with very similar unit cells, the symmetric and asymmetric stretching frequencies for the Rb species are 8.5 and 6.8 cm^{-1} higher than those of the Cs compound, respectively.[20] In compounds **3** and **6**, the changes in the properties of the cation are significantly smaller than those found when using alkali metal cations.

When comparing the infrared and Raman spectra of compounds **3** and **6**, the asymmetric stretching frequencies (ν_3) are identical for the two species, and the symmetric stretches (ν_1) vary only by 1 cm^{-1}, which is within the error of the spectrometer (Figure 3, Table 4). Additionally, both the stretching and interaction force constants are almost identical for compounds **3** and **6**, showing that, if the minor differences in size and charge distribution between the PPh_4^+ and $AsPh_4^+$ do slightly vary in their influence on the uranyl moiety, these differences are too small to be detected using Raman and infrared spectroscopy. This result combined with our investigation into lattice solvent influences and our previous work with alkali metal cations[20] shows that, while we are able use Raman and infrared spectroscopy to investigate the influences on the vibrational spectra (and therefore electronic structure of the uranyl) from the secondary coordination sphere, this technique is not sensitive enough to distinguish between very minor changes in the cation, such as those seen when moving between PPh_4^+ and $AsPh_4^+$.

Effect of Desolvation. The effects of lattice solvent on the uranyl symmetric stretching mode can also be observed by following the desolvation of **3**, **4**, and **6** using Raman spectroscopy. For compounds **3** (CH_2Cl_2) and **6** (CH_2Cl_2), probing a single crystal freshly isolated from the mother liquor produces an initial spectrum exhibiting the ν_1 symmetric

dx.doi.org/10.1021/ic501553m | Inorg. Chem. 2014, 53, 11036−11045

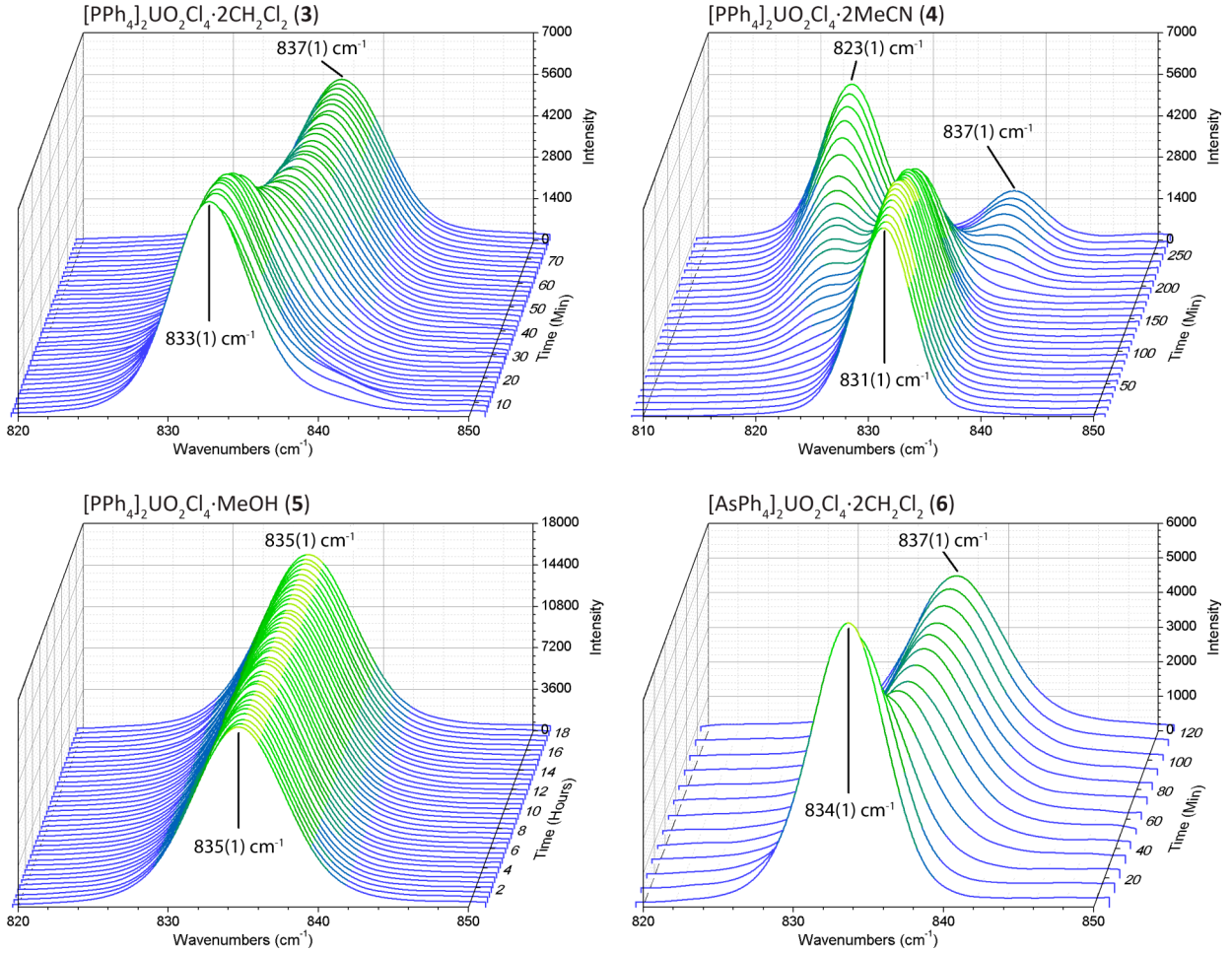

Figure 5. Raman spectra depicting changes in the uranyl symmetric stretching frequency over time for $[PPh_4]_2UO_2Cl_4{\cdot}2CH_2Cl_2$ (**3**) (upper left, spectra are every 2 min, 4−78 min), $[PPh_4]_2UO_2Cl_4{\cdot}2MeCN$ (**4**) (upper right, spectra are every 10 min, 0−270 min), $[PPh_4]_2UO_2Cl_4{\cdot}MeOH$ (**5**) (lower left, spectra are every 30 min, 0−18 h), and $[AsPh_4]_2UO_2Cl_4{\cdot}2CH_2Cl_2$ (**6**) (lower right, spectra are every 10 min, 0−120 min). All spectra for compounds **3**, **4**, and **6** were normalized to the prominent PPh_4^+ signal around 1000 cm^{-1}, while the spectra for **5** were normalized to the signal at 112 cm^{-1}.

stretching mode at 833(1) and 834(1) cm^{-1}, respectively (Figure 5). In both cases, the symmetric stretch undergoes a blue-shift over a period of 80 min for **3** and 120 min for **6**, resulting in signals at 837 cm^{-1}. These new uranyl symmetric stretching signals, resulting from the desolvation of **3** and **6**, are consistent with the unsolvated species $[PPh_4]_2UO_2Cl_4$ ($P\bar{1}$) (**1**) (Table 4). Additionally, signals corresponding to the scissoring ($\delta(CCl_2)$ = 283 cm^{-1}) and symmetric stretching ($\nu_s(CCl_2)$ = 704 cm^{-1}) of the CCl_2 moiety in dichloromethane[53] decrease significantly over the same time frame (Figures S3−S5).

Compound **4** (MeCN) appears to be slightly more stable than the CH_2Cl_2 solvates and undergoes desolvation of the lattice solvent over a period of 4.5 h. As the intensity of the initial uranyl symmetric stretch at 831(1) cm^{-1} decreases over 4.5 h, two new ν_1 signals grow in at 837(1) and 823(1) cm^{-1} that may correspond to the unsolvated species **1** and **2**, respectively, though we do not have any indication as to the identity of the crystallographic phase. Concurrent with the reduction in the symmetric stretch of **4**, signals corresponding to MeCN[72,73] located near 380 (ν_8, C−C−N bend), 750 ($2\nu_8$), and 920 (ν_4, C−C stretch) cm^{-1} also disappear, indicating the release of the lattice solvent and conversion to an unsolvated species.

During the desolvation of compounds **3**, **4**, and **6**, shifting of the -yl symmetric stretch concomitant with the significant decrease of the solvent signals indicates that unbound solvent within the crystal lattice influences the frequency of the uranyl ν_1 symmetric stretch. While this influence is relatively small, with the largest shift being about 8 cm^{-1} during the desolvation of **4**, it shows that lattice solvent in the secondary coordination sphere of the uranium atom may indirectly influence the uranyl moiety. As was seen in the solid-state molecular structure, this correlation is spectroscopic evidence for the presence of hydrogen-bonding between the uranyl anion and the unbound solvent in the crystal lattice. Compound **5** appears to be more stable than the other solvated species and does not exhibit evidence of desolvation over 18 h.

Comparison of $Rb_2UO_2Cl_4{\cdot}2H_2O$ ($P\bar{1}$) and $Rb_2PuO_2Cl_4$ ($C2/m$). Using the results from this investigation, we can now revisit the data from our previous work and make some qualitative assessments about how the spectroscopic data for $Rb_2UO_2Cl_4{\cdot}2H_2O$ ($P\bar{1}$) (**U-Rb**) and $Rb_2PuO_2Cl_4$ ($C2/m$) (**Pu-Rb**) fit within the patterns drawn from the Cs and Me_4N analogues.[20] Using the comparison of compounds **1** and **2** performed above, we know that the crystallographic phase of the compound can influence the uranyl ν_1 symmetric and ν_3 asymmetric stretching frequencies of the compound by as much

dx.doi.org/10.1021/ic501553m | Inorg. Chem. 2014, 53, 11036−11045

as 14 cm^{-1} and perhaps more. Additionally, our comparison of compounds **1**, **3**, and **4** demonstrates that the presence of lattice solvent can cause a shift in the uranyl symmetric and asymmetric stretching frequencies.

In our previous work, we experimentally determined that the ν_1 symmetric/ν_3 asymmetric stretching frequencies for **U-Rb** and **Pu-Rb** are located at 839/907 cm^{-1} and 810/932 cm^{-1}, respectively.[20] Within our observations made for the Cs and Me_4N analogues, the symmetric stretch red-shifted and the asymmetric stretch either blue-shifted or stayed the same when the actinide metal center was changed from uranium to plutonium. Additionally, the influences from the crystallographic phase and lattice solvent of **U-Rb** help to account for the 25 cm^{-1} red-shift of the asymmetric stretching frequency in comparison to **Pu-Rb**, whereas the largest metal-centric shift for the Cs and Me_4N analogues is only 3 cm^{-1}. The sensitivity of the actinyl vibrational frequencies to both crystallographic phase and more distant chemical environments suggests that, when comparing vibrational frequencies among the same actinide and between actinides, a great deal of caution must be afforded, particularly when making inferences in regard to bond distances and bond strengths.

CONCLUSION

We have presented the crystallographic and spectroscopic characterization for a series of uranyl tetrachloride compounds. Analysis of the uranyl symmetric and asymmetric stretching frequencies has shown that the electronic structure of the UO_2^{2+} moiety is influenced by both the crystallographic phase and the presence of lattice solvent. By calculating the stretching and interaction force constants for the uranyl moiety, we have quantified these influences and shown that, for this system, the crystallographic phase of the compound has a significantly greater effect upon the uranyl vibrational spectra than the presence of lattice solvent. We have also used the force constant calculations to show that changes in the vibrational properties of the uranyl, possibly resulting from minor differences in the cation, such as exchanging $AsPh_4^+$ for PPh_4^+, are too small to be measured using Raman and infrared spectroscopy. Additionally, we have followed the desolvation of the CH_2Cl_2 and MeCN solvated compounds by Raman spectroscopy and shown that, upon the loss of lattice solvent, the resulting symmetric stretching frequencies are consistent with crystallographically characterized unsolvated species. We were able to use our results from this study to qualitatively analyze the spectroscopic data for our previously reported compounds, $Rb_2UO_2Cl_4{\cdot}2H_2O$ ($P\bar{1}$) and $Rb_2PuO_2Cl_4$ ($C2/m$), which vary by actinide metal, space group, and the presence of lattice solvent. In future studies, we aim to continue exploring the actinyl moiety through Raman and infrared spectroscopy. We will use the knowledge obtained in this study to more accurately analyze trends across the actinide series, and we urge caution when making generalized conclusions from comparison of actinyl vibrational frequencies.

ASSOCIATED CONTENT

Supporting Information

Detailed synthetic procedures, additional vibrational analysis, crystallographic information in CIF format, solid-state molecular structures with 50% probability ellipsoids, IR (400−4000 cm^{-1}) spectra, ATR spectra (~550−4000 cm^{-1}), and Raman spectra (100−4000 cm^{-1}) for the reported complexes. This material is available free of charge via the Internet at http://pubs.acs.org.

AUTHOR INFORMATION

Corresponding Author

*E-mail: rewilson@anl.gov.

Notes

The authors declare no competing financial interest.

ACKNOWLEDGMENTS

This work was performed at Argonne National Laboratory, operated for the United States Department of Energy, Office of Science, Office of Basic Energy Sciences, by UChicagoArgonne LLC under contract number DE-AC02-06CH11357.

REFERENCES

(1) Cotton, F. A.; Wilkinson, G.; Murillo, C. A.; Bochmann, M. *Advanced Inorganic Chemistry*, 6th ed.; Wiley: New York, 1999.
(2) Cotton, S. *Lanthanide and Actinide Chemistry*; John Wiley and Sons, Ltd.: Chichester, 2006.
(3) Gaunt, A. J.; Neu, M. P. *C. R. Chim.* **2010**, *13* (6−7), 821−831.
(4) Jones, M. B.; Gaunt, A. J. *Chem. Rev.* **2012**, *113* (2), 1137−1198.
(5) Seaborg, G. T. *Chem. Eng. News* **1945**, *23*, 2190−2193.
(6) Seaborg, G. T. *Science* **1946**, *104* (2704), 379−386.
(7) Seaborg, G. T. Paper 21.1: Electronic Structure of the Heaviest Elements. In *The Transuranium Elements: Research Papers*; McGraw-Hill Book Co. Inc.: New York, 1949; Vol. *2*.
(8) Allen, P. G.; Bucher, J. J.; Shuh, D. K.; Edelstein, N. M.; Craig, I. *Inorg. Chem.* **2000**, *39* (3), 595−601.
(9) Andreev, G.; Budantseva, N.; Fedoseev, A.; Moisy, P. *Inorg. Chem.* **2011**, *50* (22), 11481−11486.
(10) Apostolidis, C.; Schimmelpfennig, B.; Magnani, N.; Lindqvist-Reis, P.; Walter, O.; Sykora, R.; Morgenstern, A.; Colineau, E.; Caciuffo, R.; Klenze, R.; Haire, R. G.; Rebizant, J.; Bruchertseifer, F.; Fanghänel, T. *Angew. Chem., Int. Ed.* **2010**, *49* (36), 6343−6347.
(11) Brendebach, B.; Banik, N. L.; Marquardt, C. M.; Rothe, J.; Denecke, M.; Geckeis, H. *Radiochim. Acta* **2009**, *97* (12), 701−708.
(12) D'Angelo, P.; Spezia, R. *Chem.—Eur. J.* **2012**, *18* (36), 11162−11178.
(13) Diamond, R. M.; Street, K.; Seaborg, G. T. *J. Am. Chem. Soc.* **1954**, *76* (6), 1461−1469.
(14) Hennig, C.; Ikeda-Ohno, A.; Tsushima, S.; Scheinost, A. C. *Inorg. Chem.* **2009**, *48* (12), 5350−5360.
(15) Hennig, C.; Kraus, W.; Emmerling, F.; Ikeda, A.; Scheinost, A. C. *Inorg. Chem.* **2008**, *47* (5), 1634−1638.
(16) Hennig, C.; Schmeide, K.; Brendler, V.; Moll, H.; Tsushima, S.; Scheinost, A. C. *Inorg. Chem.* **2007**, *46* (15), 5882−5892.
(17) Jones, M. B.; Gaunt, A. J.; Gordon, J. C.; Kaltsoyannis, N.; Neu, M. P.; Scott, B. L. *Chem. Sci.* **2013**, *4* (3), 1189−1203.
(18) Schnaars, D. D.; Batista, E. R.; Gaunt, A. J.; Hayton, T. W.; May, I.; Reilly, S. D.; Scott, B. L.; Wu, G. *Chem. Commun.* **2011**, *47* (27), 7647−7649.
(19) Schnaars, D. D.; Gaunt, A. J.; Hayton, T. W.; Jones, M. B.; Kirker, I.; Katsoyannis, N.; May, I.; Reilly, S. D.; Scott, B. L.; Wu, G. *Inorg. Chem.* **2012**, *51* (15), 8557−8566.
(20) Schnaars, D. D.; Wilson, R. E. *Inorg. Chem.* **2013**, *52* (24), 14138−14147.
(21) Schnaars, D. D.; Wilson, R. E. *Inorg. Chem.* **2012**, *51* (17), 9481−9490.
(22) Sokolova, M. N.; Fedosseev, A. M.; Andreev, G. B.; Budantseva, N. A.; Yusov, A. B.; Moisy, P. *Inorg. Chem.* **2009**, *48* (19), 9185−9190.
(23) Tait, C. D.; Donohoe, R. J.; Clark, D. L.; Conradson, S. D.; Ekberg, S. A.; Keogh, D. W.; Neu, M. P.; Reilly, S. D.; Runde, W. H.; Scott, B. L. *Actinide Research Quarterly*; Report LA-LP-04-60, Los Alamos National Laboratory, 2004; Vol. *1*, pp 20−22.
(24) Wilson, R. E. *Inorg. Chem.* **2011**, *50* (12), 5663−5670.
(25) Wilson, R. E. *Inorg. Chem.* **2012**, *51* (16), 8942−8947.

(26) Hay, P. J.; Martin, R. L.; Schreckenbach, G. *J. Phys. Chem. A* **2000**, *104* (26), 6259−6270.
(27) Kaltsoyannis, N. *Inorg. Chem.* **2012**, *52* (7), 3407−3413.
(28) Kirker, I.; Kaltsoyannis, N. *Dalton Trans.* **2011**, *40* (1), 124−131.
(29) Réal, F.; Vallet, V.; Clavaguéra, C.; Dognon, J.-P. *Phys. Rev. A* **2008**, *78* (5), 052502.
(30) *Bruker APEX2 Software Suite*, APEX2 v2011.4−1; Bruker AXS: Madison, WI, 2011.
(31) Duval, P. B.; Burns, C. J.; Buschmann, W. E.; Clark, D. L.; Morris, D. E.; Scott, B. L. *Inorg. Chem.* **2001**, *40* (22), 5491−5496.
(32) Gatto, C. C.; Schulz Lang, E.; Kupfer, A.; Hagenbach, A.; Abram, U. *Z. Anorg. Allg. Chem.* **2004**, *630* (8−9), 1286−1295.
(33) Leverd, P. C.; Rinaldo, D.; Nierlich, M. *J. Chem. Soc., Dalton Trans.* **2002**, *6*, 829−831.
(34) Spencer, L. P.; Yang, P.; Minasian, S. G.; Jilek, R. E.; Batista, E. R.; Boland, K. S.; Boncella, J. M.; Conradson, S. D.; Clark, D. L.; Hayton, T. W.; Kozimor, S. A.; Martin, R. L.; MacInnes, M. M.; Olson, A. C.; Scott, B. L.; Shuh, D. K.; Wilkerson, M. P. *J. Am. Chem. Soc.* **2013**, *135* (6), 2279−2290.
(35) Anson, C. E.; AlJowder, O.; Jayasooriya, U. A.; Powell, A. K. *Acta Crystallogr.* **1996**, *C52*, 279−281.
(36) Hall, D.; Rae, A. D.; Waters, T. N. *Acta Crystallogr.* **1966**, *20*, 160−162.
(37) Watkin, D. J.; Denning, R. G.; Prout, K. *Acta Crystallogr.* **1991**, *C47*, 2517−2519.
(38) Brown, D. R.; Chippindale, A. M.; Denning, R. G. *Acta Crystallogr.* **1996**, *C52*, 1164−1166.
(39) Bohrer, R.; Conradi, E.; Müller, U. *Z. Anorg. Allg. Chem.* **1988**, *558* (1), 119−127.
(40) Crawford, M.-J.; Mayer, P. *Inorg. Chem.* **2005**, *44* (16), 5547−5549.
(41) Bois, C.; Dao, N. Q.; Rodier, N. *Acta Crystallogr.* **1976**, *B32*, 1541−1544.
(42) Bombieri, G.; Forsellini, E.; Graziani, R. *Acta Crystallogr.* **1978**, *B34* (8), 2622−2624.
(43) Rogers, R. D.; Kurihara, L. K.; Benning, M. M. *Inorg. Chem.* **1987**, *26* (26), 4346−4352.
(44) Taylor, J. R. *An Introduction to Error Analysis: The Study of Uncertainties in Physical Measurements*; University Science Books: Sausalito, CA, 1997.
(45) Franczyk, T. S.; Czerwinski, K. R.; Raymond, K. N. *J. Am. Chem. Soc.* **1992**, *114* (21), 8138−8146.
(46) Braga, D.; Grepioni, F. *New J. Chem.* **1998**, *22* (11), 1159−1161.
(47) Brammer, L.; Bruton, E. A.; Sherwood, P. *Cryst. Growth Des.* **2001**, *1* (4), 277−290.
(48) Steiner, T. *Acta Crystallogr.* **1998**, *B54* (4), 456−463.
(49) Goicoechea, J. M.; Mahon, M. F.; Whittlesey, M. K.; Kumar, P. G. A.; Pregosin, P. S. *Dalton Trans.* **2005**, *3*, 588−597.
(50) Zhang, Q. A.; He, L. S.; Liu, J. M.; Wang, W.; Zhang, J. Y.; Su, C. Y. *Dalton Trans.* **2010**, *39* (46), 11171−11179.
(51) Bagnall, K. W.; du Preez, J. G. H.; Gellatly, B. J.; Holloway, J. H. *J. Chem. Soc., Dalton Trans.* **1975**, *0* (19), 1963−1968.
(52) Day, J. P.; Venanzi, L. M. *J. Chem. Soc. A* **1966**, 1363−1367.
(53) Nakamoto, K. *Infrared and Raman Spectra of Inorganic and Coordination Compounds Part A: Theory and Applications in Inorganic Chemistry*, 5th ed.; John Wiley & Sons, Inc.: New York, 1997.
(54) Jones, L. H.; Penneman, R. A. *J. Chem. Phys.* **1953**, *21* (3), 542−544.
(55) Flint, C. D.; Tanner, P. A. *J. Chem. Soc., Faraday Trans. 2* **1978**, *74*, 2210−2217.
(56) Flint, C. D.; Tanner, P. A. *J. Chem. Soc., Faraday Trans. 2* **1981**, *77* (10), 1865−1878.
(57) Flint, C. D.; Tanner, P. A. *Mol. Phys.* **1981**, *44* (2), 411−425.
(58) Gál, M.; Goggin, P. L.; Mink, J. *Spectrochim. Acta A* **1992**, *48* (1), 121−132.
(59) Newbery, J. E. *Spectrochim. Acta A* **1969**, *25* (10), 1699−1702.
(60) Ohwada, K. *Spectrochim. Acta A* **1975**, *31* (7), 973−977.
(61) Ohwada, K. *J. Inorg. Nucl. Chem.* **1978**, *40* (7), 1369−1374.
(62) Ohwada, K. *Appl. Spectrosc.* **1980**, *34* (3), 327−331.
(63) Marzotto, A. *Inorg. Nucl. Chem. Lett.* **1974**, *10* (10), 915−923.
(64) Wilkins, R. W. T. *Z. Kristallogr.* **1971**, *134* (3−4), 285−290.
(65) Allen, P. G.; Bucher, J. J.; Clark, D. L.; Edelstein, N. M.; Ekberg, S. A.; Gohdes, J. W.; Hudson, E. A.; Kaltsoyannis, N.; Lukens, W. W.; Neu, M. P.; Palmer, P. D.; Reich, T.; Shuh, D. K.; Tait, C. D.; Zwick, B. D. *Inorg. Chem.* **1995**, *34* (19), 4797−4807.
(66) Fillaux, C.; Guillaumont, D.; Berthet, J.-C.; Copping, R.; Shuh, D. K.; Tyliszczak, T.; Auwer, C. D. *Phys. Chem. Chem. Phys.* **2010**, *12* (42), 14253−14262.
(67) Fortier, S.; Hayton, T. W. *Coord. Chem. Rev.* **2010**, *254* (3−4), 197−214.
(68) Ingram, K. I. M.; Haller, L. J. L.; Kaltsoyannis, N. *Dalton Trans.* **2006**, No. 20, 2403−2414.
(69) McGlynn, S. P.; Smith, J. K.; Neely, W. C. *J. Chem. Phys.* **1961**, *35* (1), 105−116.
(70) Vallet, V.; Wahlgren, U.; Grenthe, I. *J. Phys. Chem. A* **2012**, *116* (50), 12373−12380.
(71) Wilson, R. E.; Schnaars, D. D.; Andrews, M. B.; Cahill, C. L. *Inorg. Chem.* **2013**, *53* (1), 383−392.
(72) Addison, C. C.; Amos, D. W.; Sutton, D. *J. Chem. Soc. A* **1968**, 2285−2290.
(73) Neelakantan, P. *Proc. Indian Acad. Sci.* **1964**, *60* (6), 422−424.